Profile Equations for Film Flows at Moderate Reynolds Numbers

An approximate equation for the evolution of finite-amplitude, long disturbances to Newtonian liquid films is found to be accurate over a wide range of Reynolds numbers. A long-wave expansion leads to a film profile equation asymptotically correct when wave number and Reynolds number are small. Solutions of the film profile equation are compared to exact and other approximate solutions of the Navier-Stokes system. An alternative form of the film profile equation results in remarkably accurate solutions, when Reynolds numbers are moderate, in the cases of standing or monotonically decaying waves in horizonatal films, rising film flow, final acceleration of a moving film, and film flow emerging from a slot coater.

Haroon S. Kheshgi
Corporate Research Laboratories
Exxon Research
and Engineering Company
Annandale, NJ 08801

Introduction

Disturbances to liquid films which are long compared to the depth of the film are of common interest in coating flow applications. To analyze such situations a long-wave expansion can be made to eliminate the dimension normal to the film substrate from the Navier-Stokes system and arrive at an approximate equation for the dependence of film profile on time and spatial dimensions tangential to the substrate. When applied to an inviscid film, a long-wave expansion leads to shallow water equations (Airy, 1845), the Boussinesq equation (1871), or the Korteweg deVries equation (1895). For highly viscous films, the expansion to lowest order is equivalent to the lubrication approximation and has been used to analyze a variety of film flow phenomena (see, e.g., Landau and Levich, 1942; Ruschak, 1978; Higgins and Scriven, 1979; Kheshgi and Scriven, 1979; Teletzke, 1983; Kheshgi, 1984; Gauglitz and Radke, 1988; Kheshgi and Scriven, 1988).

Higher-order terms, which include the effect of inertia, lead to a film profile equation that has been used to determine the stability of liquid films on inclined substrates and follow the finite-amplitude disturbances that ensue (see, e.g., Benney, 1966; Roskes, 1970; Gjevik, 1970; Krantz and Goren, 1970; Nakaya, 1975; Atherton and Homsy, 1976; Petviashvili and Tsvelodub, 1978). A characteristic of the inclined-film problem is that disturbances which have been of interest are ones near the point of neutral stability, and the Reynolds number of neutrally-stable waves of small wave number is small (except for the case of very nearly horizontal films). Interestingly, the long-wave expansion has not been used to investigate other film flow situations that are of industrial and academic interest when the magnitude of inertia is comparable to that of viscous forces, which in this context is defined as situations at moderate Reynolds numbers. The form of the film profile equation used to study disturbances to inclined films is found to be inaccurate in such situations. In these situations, the alternative form of the film profile equation found here proves useful.

Several approximation (not asymptotic) methods have been used to include the effects of inertia in film profile equations based on the lubrication approximation (e.g., Tallmadge and Sorka, 1969; Spiers et al., 1974; Esmail and Hummel, 1975). Most notably, Cerro and Scriven (1979), as well as Ruschak (1978) and Kheshgi (1984), used an approximate (parabolic) velocity profile in a liquid film along with an integral form of the Navier-Stokes system (Higgins and Scriven, 1979) to arrive at a film profile equation that gave roughly the right behavior for several coating flows they examined. The discovery of the alternative form was the result of an effort to improve upon the film profile equations proposed by Cerro and Scriven (1979). The alternative form of the film profile equation found here is similar to that of Cerro and Scriven (1979) except that it includes the effect of inertia by means of an asymptotic expansion and, based on comparisons, is more accurate away from the small Reynolds number asymptotic limit.

A long-wave expansion is applied to a two-dimensional film flow on a flat substrate to arrive at a film profile equation with one spatial dimension. The derivation of film profile equations for three-dimensional film flows, that may be on curved surfaces, has been reported elsewhere (e.g., Roskes, 1970; Atherton and Homsy, 1976; Kheshgi, 1984). The first two terms in the expansion in wave number are included. The driving forces of capillary pressure and gravity are included in the lowest-order term in the expansion. Including only terms of lowest order results in an equation balancing the driving forces with viscous shear. Including terms of the next order in magnitude results in a film profile equation accounting for the effect of inertia.

Solutions of film profile equations based on the long-wave expansion are compared to exact and other approximate (Cerro and Scriven, 1979) solutions of the Navier-Stokes system for cases depicted in Figure 1. It was found that the film profile equation with a form like that used to study the evolution of disturbances to flow down an inclined plate leads to indefinite (unrealistic) solutions at finite Reynolds number. For the test cases examined, an *alternative* form of the film profile equation is found to lead to accurate solutions, although not asymptotically, as the effect of inertia becomes comparable or larger than the effect of viscous shear. Discussed in this article are the reasons behind the improved accuracy of the alternative form of the film profile equation and a generalization of the alternative form.

Long-Wave Expansion for Viscous Film Flows

This section reports on a derivation of a film profile equation following the long-wave expansion used by Benney (1966) for the analysis of the stability of inclined films. The derivation, however, differs from Benney's in two important respects. First, the driving forces of capillary pressure and gravity, both normal and tangent to the film, are all included in the lowest-order term in the expansion. This allows analysis of situations where the component of gravity tangent to the film is *not* the dominant driving force, as it is when examining the stability of inclined films. Second, following Ruschak (1978), the full curvature expression in the normal stress boundary condition is not approximated, allowing the resulting film profile equation to give composite solutions of those of the Young-Laplace equation and a long-wave expansion-based film profile equation.

The Navier-Stokes system is made dimensionless by choosing two length scales: a characteristic film thickness, h_o, and a characteristic disturbance length ℓ. The dimensional (primed) variables are made dimensionless by the appropriate choice of stretched units given by:

$$x' = \ell x, \quad y' = h_o y, \quad h' = h_o h, \quad t' = (\ell/U)t,$$
$$u' = Uu, \quad v' = \alpha U v, \quad p' = (\mu U/h_o \alpha)p. \tag{1}$$

The characteristic velocity for the situation of interest is U. The dimensionless wave number $\alpha \equiv h_o/\ell$ is small in many applications.

The equation for the conservation of momentum when separated into its components normal and tangent to the solid substrate are:

$$\alpha^3 Re(v_t + uv_x + vv_y) = -p_y + \alpha^4 v_{xx} + \alpha^2 v_{yy} + \alpha St g_j$$
$$\alpha Re(u_t + uu_x + vu_y) = -p_x + \alpha^2 u_{xx} + u_{yy} + St g_i. \tag{2}$$

The Reynolds number $Re \equiv \rho U h_o/\mu$. The inverse Stokes number $St \equiv h_o^2 \rho g/\mu U$. The x and y components of the unit gravity

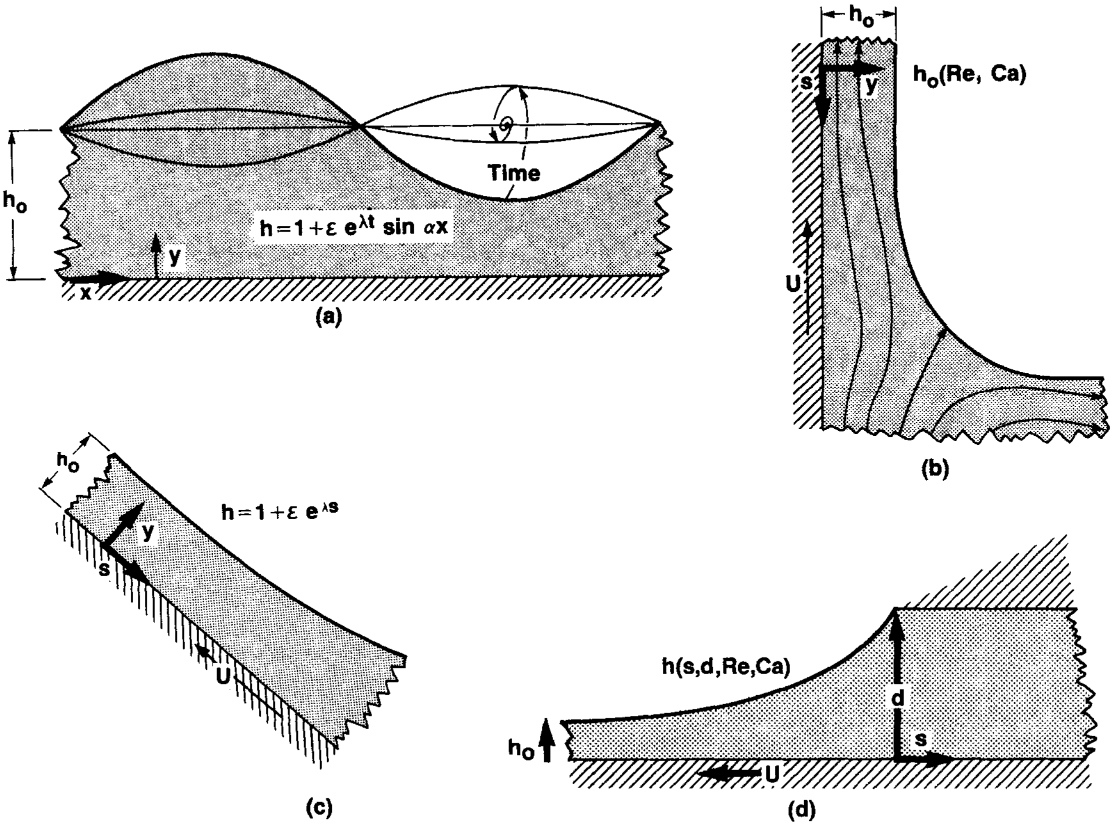

Figure 1. Evolution of liquid film profiles in situations of: (a) disturbances to horizontal films; (b) rising film flow; (c) final acceleration of a liquid film; and (d) a film emerging from a slot coater.

vector are g_i and g_j, respectively. The continuity equation contains no small parameter α:

$$u_x + v_y = 0. \tag{3}$$

The integral form of the kinematic condition is:

$$h_t = -\frac{\partial}{\partial x}\left(\int_0^h u\, dy\right). \tag{4}$$

At the underlying solid substrate, the no-slip, no-penetration boundary conditions are presumed:

$$u = v = 0. \tag{5}$$

The normal and tangential stress conditions at the free surface (Higgins and Scriven, 1979) are:

$$\alpha^{-1}p - 2\alpha v_y - \alpha h_x(\alpha^2 v_x + u_y) + \alpha^2 Ca^{-1} 2\boldsymbol{H} = 0, \tag{6}$$

$$(\alpha^2 h_x^2 - 1)(\alpha^2 v_x + u_y) + 2\alpha^2 h_x(u_x - v_y) = 0, \tag{7}$$

where the mean curvature of the free surface is $\boldsymbol{H}$, and the capillary number is $Ca \equiv \mu U/\sigma$.

The system of Eqs. 2–7 is approximated by a profile equation by expanding velocities and pressure as a series in the small parameter α:

$$u = u^{(0)} + \alpha u^{(1)} + \alpha^2 u^{(2)} + 0(\alpha^3),$$

$$v = v^{(0)} + \alpha v^{(1)} + \alpha^2 v^{(2)} + 0(\alpha^3),$$

$$p = p^{(0)} + \alpha p^{(1)} + \alpha^2 p^{(2)} + 0(\alpha^3). \tag{8}$$

When only terms of 0(1) are retained, the zeroth-order equation system results:

$$0 = -p_y^{(0)} + \alpha\, St\, g_j \tag{9}$$

$$0 = -p_x^{(0)} + u_{yy}^{(0)} + St\, g_i \tag{10}$$

$$u_x^{(0)} + v_y^{(0)} = 0 \tag{11}$$

$$h_t = -\left(\int_0^h u^{(0)}\, dy\right)_x \tag{12}$$

$$u^{(0)} = v^{(0)} = 0 \quad \text{at} \quad y = 0 \tag{13}$$

$$u_y^{(0)} = 0 \quad \text{at} \quad y = h \tag{14}$$

$$p^{(0)} + \alpha^3 Ca^{-1}\, 2\boldsymbol{H} = 0 \quad \text{at} \quad y = h \tag{15}$$

The parameter groups $\alpha\, St\, g_j$, $St\, g_i$, and $\alpha^3\, Ca^{-1}$ are measures of the three driving forces, and their magnitudes are determined by the four independent parameters, g_i/g_j (a measure of the inclination of the substrate), St, Ca, and α. Each is treated as if it were of 0(1), even though two contain powers of α, because any of the three could dominate in different situations. Appropriate choice of U and ℓ (and therefore α) leads to at least one of the parameter groups to be 0(1) and the remaining parameter groups to be smaller (negligible). From the y-momentum equation (Eq. 9) and the normal stress condition (Eq. 15), $p^{(0)}$ is found:

$$p^{(0)} = (y - h)\alpha\, St\, g_j - \alpha^3 Ca^{-1} 2\boldsymbol{H}. \tag{16}$$

Velocity $u^{(0)}$ is found from the x-momentum equation (Eq. 10) and conditions (Eqs. 13 and 14):

$$u^{(0)} = F \cdot (yh - y^2/2), \tag{17}$$

where the driving force F is defined as

$$F \equiv St\, g_i + \alpha\, St\, g_j\, h_x + \alpha^3\, Ca^{-1}(2\boldsymbol{H})_x. \tag{18}$$

Other driving forces, such as electromagnetic force or the long-range molecular forces that cause disjoining pressure (Teletzke, 1983), can also be included in F. Retention of the full expression for surface curvature allows accurate solution of situations where surface curvature may be great, yet the effects of viscous or inertial forces, which would not be represented accurately by a long-wave expansion, are negligible. This approach has been used by Ruschak (1978) to analyze a film flowing down to a liquid pool, Kheshgi and Scriven (1979, see also Kheshgi, 1984) for rising film flow shown in Figure 1b, Teletzke (1983) for bubbles moving through capillary tubes, and Gauglitz and Radke (1988) for collar formation in annular films. It results, in essence, in a composite solution between that of a lubrication-type film profile equation and the Young-Laplace equation. Now that $u(0)$ is represented as a function of h and y alone by Eqs. 17–18, the kinematic condition (Eq. 12) gives an equation for the film profile:

$$h_t = -(h^3 F)_x/3. \tag{19}$$

Solutions of this film profile equation are accurate to an error of $0(\alpha^2 + \alpha Re)$.

Higher-order terms can be retained to include the effect of viscous normal stress and fluid inertia. The 0(1) system above balances only viscous shear stress with the driving forces. Balancing terms of $0(\alpha)$ leaves an equation system for $u^{(1)}$, $v^{(1)}$, and $p^{(1)}$ and a more accurate equation for film profile h:

$$0 = -p_y^{(1)} \tag{20}$$

$$Re[u_t^{(0)} + u^{(0)}u_x^{(0)} + v^{(0)}u_y^{(0)}] = -p_x^{(1)} + u_{yy}^{(1)} \tag{21}$$

$$u_x^{(1)} + v_y^{(1)} = 0 \tag{22}$$

$$h_t = -\left(\int_0^h u^{(0)} + \alpha u^{(1)}\, dy\right)_x \tag{23}$$

$$u^{(1)} = v^{(1)} = 0 \quad \text{at} \quad y = 0 \tag{24}$$

$$u_y^{(1)} = 0 \quad \text{at} \quad y = h \tag{25}$$

$$p^{(1)} = 0 \quad \text{at} \quad y = h. \tag{26}$$

The remains of the y-momentum equation (Eq. 20) are integrated over film thickness to show $p^{(1)}$ equal to the constant of integration; the normal stress condition (Eq. 26) determines that constant, and therefore $p^{(1)}$, to be simply zero. The x-momentum equation (Eq. 21) is integrated twice over the film thickness to express $u^{(1)}$—after application of the conditions, Eqs. 24 and 25, as the lower bounds of the following double integral—as a function of h and a polynomial of y:

$$u^{(1)} = Re \int_0^y \int_h^y [u_t^{(0)} + u^{(0)}u_x^{(0)} + v^{(0)}u_y^{(0)}]\, dy^2$$

$$= Re\, F_t \left(\frac{1}{6}y^3h - \frac{1}{24}y^4 - \frac{1}{3}h^3y\right)$$

$$+ Re\, Fh_t \left(\frac{1}{6}y^3 - \frac{1}{2}h^2y\right)$$

$$+ Re\, FF_x \left(\frac{1}{360}y^6 - \frac{1}{60}y^5h + \frac{1}{24}h^2y^4 - \frac{1}{10}h^5y\right)$$

$$+ Re\, F^2h_x \left(\frac{1}{24}y^4h - \frac{1}{6}h^4y\right). \qquad (27)$$

Inserting Eqs. 17 and 27 into kinematic condition (Eq. 23) gives

$$h_t = -\left(\frac{h^3}{3}F\right)_x + \alpha Re\left(\frac{2}{15}h^5F_t + \frac{5}{24}h^4h_tF + \frac{37}{840}h^7FF_x + \frac{3}{40}h^6h_xF^2\right)_x, \qquad (28)$$

a film profile equation including the effect of inertia as a perturbation to system (Eqs. 9–15), a balance between viscous shear and the driving forces. This equation can be simplified—with, however, loss of generality—to that derived by Krantz and Goren (1970). Profile equation (Eq. 28) for the single unknown h is accurate to an error to $0(\alpha^2 + \alpha^2Re^2)$. As will be seen in the next section, Eq. 28 leads to low-accuracy solutions when αRe, a measure of the effect of inertia, is large. Also demonstrated in the next section, however, is that an alternative form of Eq. 28 yields accurate solutions when αRe is large and α is small, and asymptotically accurate solutions—as does Eq. 28—when αRe and α are small.

Accuracy of Film Profile Equations at Moderate and High-Reynolds Number

Infinitesimal disturbances to horizontal films

The evolution of sinusoidal disturbances to a horizontal film, as shown in Figure 1a, is a convenient case to test the accuracy of film profile equations.

In the limit of small amplitude ϵ, the evolution of sinusoidal disturbances of wavenumber α (note that stretching Eq. 1 still applies) to horizontal liquid films follows the *exact* solution

$$h = 1 + \epsilon e^{\lambda t} \sin(x). \qquad (29)$$

The wave growth rates λ are the roots of the equation (Wehausen and Laitone, 1960):

$$(\gamma^2 + \alpha^2)^2 \frac{(\gamma^2 + \alpha^2)[\gamma \cosh(\gamma)\cosh(\alpha) - \alpha \sinh(\gamma)\sinh(\alpha)] - 2\alpha^2\gamma}{(\gamma^2 + \alpha^2)[\gamma\cosh(\gamma)\sinh(\alpha) - \alpha\sinh(\gamma)\cosh(\alpha)]}$$

$$- 4\alpha^3\gamma \frac{2\alpha[\alpha\cosh(\alpha)\cosh(\gamma) - \gamma\sinh(\alpha)\sinh(\gamma)] - (\gamma^2 + \alpha^2)}{2\alpha[\alpha\cosh(\alpha)\sinh(\gamma) - \gamma\sinh(\alpha)\cosh(\gamma)]} + \alpha Re(St + \alpha^2Ca^{-1}) = 0, \qquad (30)$$

where

$$\lambda = Re^{-1}(\gamma^2 - \alpha^2).$$

This expression for λ has some simple limiting solutions. In the limit of low Reynolds number, the creeping decay rate is given by (Orchard, 1962; Kheshgi and Scriven, 1988):

$$\lambda = -\frac{1}{2}\left[\frac{\tanh(\alpha) - \alpha\,\mathrm{sech}^2(\alpha)}{\alpha^2(1 + \alpha\,\mathrm{sech}^2\alpha)}\right](St + \alpha^2Ca^{-1}). \qquad (31)$$

In the limit of high Reynolds number, the inviscid oscillation is given by (Lamb, 1945; Whitham, 1974; Kheshgi and Scriven, 1988):

$$\lambda = \pm i\left\{\left[\frac{\tanh(\alpha)}{\alpha Re}\right](St + \alpha^2Ca^{-1})\right\}^{1/2}. \qquad (32)$$

To find decay rates and oscillation frequencies outside of the above-mentioned limiting cases, Eq. 30 is solved numerically using IMSL routine ZANLYT to find roots λ at various values of Re and α. These roots result (as discussed by Lamb, 1945, article 349) in two real values of λ corresponding to the monotonic decay of the sinusoidal, infinitesimal disturbance, or a complex pair with a negative real part corresponding to a damped standing wave.

The evolution of disturbances to a horizontal film can also be described by film profile equation (Eq. 28). Since the solid substrate is orthogonal to the acceleration of gravity ($g_i = 0$, $g_j = -1$), the driving force F given by Eq. 18 simplifies to

$$F = -\alpha St\, h_x + \alpha^3Ca^{-1}(2H)_x. \qquad (33)$$

The film profile equation (Eq. 28) is linearized to give

$$h_t = -\tfrac{1}{3}F_x + \tfrac{2}{15}\alpha Re\, F_{xt}. \qquad (34)$$

Inserting solution (Eq. 29) results in

$$\lambda = \frac{\alpha^2(St + \alpha^2Ca^{-1})}{3[-1 + \tfrac{2}{15}Re\alpha^2(St + \alpha^2Ca^{-1})]}, \qquad (35)$$

an expression for the monotonic decay of viscous films. As is evident in expression 35, it does not allow for damped standing waves, i.e., an imaginary value of λ. Furthermore, λ becomes infinite for a finite value of Reynolds number. It is clear that when $\alpha Re > 1$, the standard form of the film profile equation is useless.

The linearized film profile equation can, however, be altered by using the lower-order expression

$$h_t = -\tfrac{1}{3}F_x \qquad (36)$$

to replace derivatives of F in the inertial term resulting in a linearized version of the *alternative form* of the film profile equation:

$$h_t = -\tfrac{1}{3}F_x - \tfrac{2}{5}\alpha Re\, h_{tt}. \tag{37}$$

This results in an expression for

$$\lambda = -\frac{5}{4\,Re}\left\{1 \pm \left[1 - \frac{8}{15}Re\,\alpha^2(St + \alpha^2 Ca^{-1})\right]^{1/2}\right\}. \tag{38}$$

The growth rates λ given by Eq. 38 do exhibit a transition from a monotonic decaying disturbance (real root) to an oscillatory decaying disturbance (complex root).

Solutions resulting from the film profile equations and from the exact, infinitesimal amplitude solution can now be compared. The unit of velocity measure U, yet unspecified, is chosen so that $\alpha(St + \alpha^2 Ca^{-1}) = 1$. The growth rates (Eqs. 35 and 38) of the two forms of the film profile equations are then expressed as a simple function of Reynolds number, respectively:

$$\left(\frac{\lambda}{\alpha}\right) = \frac{1}{3\left[-1 + \frac{2}{15}(\alpha Re)\right]}, \tag{39}$$

$$\left(\frac{\lambda}{\alpha}\right) = -\frac{5}{4(\alpha Re)}\left\{1 \pm \left[1 - \frac{8}{15}(\alpha Re)\right]^{1/2}\right\}. \tag{40}$$

Several limiting comparisons are evident. At small wave number $\alpha \rightarrow 0$ and small Reynolds number $\alpha Re \rightarrow 0$, the negative real root of both Eqs. 39 and 40 with smallest magnitude real part is $\lambda = -1/3$ in agreement with Eq. 31 as it should be, since both Eqs. 39 and 40 are exact in this asymptotic limit. The result of the film profile equation (Eq. 37), along with that of the exact equation (Eq. 30), gives a second real root which becomes negative infinite as $Re \rightarrow 0$; this root can be interpreted as the deceleration of the liquid film by viscous force, which becomes immediate as Reynolds number approaches zero. At larger wave number but still zero Reynolds number, the exact solution (Eq. 31) shows a slower decay (the negative root is of smaller magnitude) than either film profile equation, due to the inclusion of normal viscous forces (cf. Kheshgi, 1984; Kheshgi and Scriven, 1988). In the limit of high Reynolds number, Eq. 39 gives a spurious result; however, Eq. 40 reduces to $\lambda/\alpha = \pm i(5/6)^{1/2}(\alpha Re)^{-1/2}$, whereas Eq. 32, in the limit of small wave number $\alpha \rightarrow 0$, reduces to $\lambda/\alpha = \pm i(\alpha Re)^{-1/2}$, an oscillation frequency a factor of 1.095 times faster than approximated by the film profile equation (Eq. 40) which surprisingly is fairly accurate far beyond the asymptotic limit where its accuracy is expected.

The real part of the two film profile equations (Eqs. 34 and 37) are contrasted in Figure 2a. The two growth rate curves—tangent near $\alpha Re = 0$—diverge as the asymptotic limit of small Reynolds number is abandoned. The transition from monotonic decay to oscillatory decay occurs where the real roots of Eq. 40 coalesce. The real and imaginary parts of film-profile-equation solution (Eq. 40) and exact infinitesimal-amplitude solution (Eq. 30) are compared in Figures 2b–c. Again, the two solutions diverge as the asymptotic limit of small Reynolds number and wave number is abandoned; however, at finite αRe and small wave number α, the film profile equation solution is a close approximation of the exact solution. In Figure 2b, a curve for $\alpha = 0.001$ is not shown because it is not discernible from that of Eq. 40, the solid line. Table 1 lists the Reynolds number αRe and growth rate λ/α at which the monotonic/oscillatory transition predicted by Eq. 30 occurs. It is comforting to note that as α becomes large the transition, Table 1, approaches an asymptotic

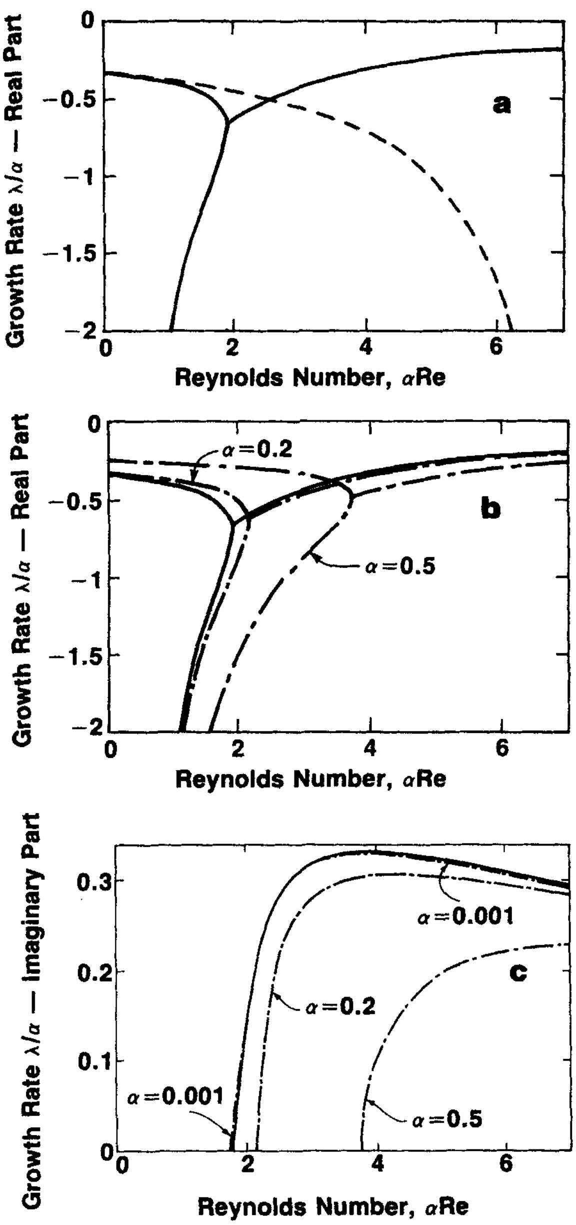

Figure 2. Growth rate of infinitesimal amplitude sinusoidal disturbances to horizontal liquid films.

(a) Predictions of the real part of the growth rate of film profile equations: ---, Eq. 34; ———, Eq. 37. The coalescence of two growth rates predicted by Eq. 37 at $\alpha Re = 15/8$ corresponds with the transition from monotonic to oscillatory decay. (b) Prediction of the real part of the growth rate of the alternative form of film profile equation: ———, Eq. 37. Exact growth rate; —·—·—, Eq. 30 at two different wave numbers. As wave number α becomes small, the film profile equation gives an accurate, but not asymptotic (except for small αRe), prediction of the growth rate. (c) Prediction of the imaginary part of the growth rate of film profile equation: ———, Eq. 37. Exact growth rate; —·—·—, Eq. 30 at three different wave numbers.

value of $\alpha^{-4}Re$, meaning the transition becomes independent of depth as α becomes large, as it should. In the limit of small wave number, film profile equation (Eq. 37) estimates the transition to be at $\alpha Re = 8/15$ and $\lambda/\alpha = 2/3$, just 1.006 and 1.004 (!) times larger than the exact solution. Predictions of the alternative form of the film profile equation are apparently not (nor are expected to be) asymptotically exact in this limit.

Table 1. Reynolds Number of the Monotonic/Oscillatory Decay Transition for Sinusoidal Disturbances of Infinitesimal Amplitude

Wave No. α	Reynolds No. αRe	$\alpha^{-4} Re$	Growth Rate λ/α
0.001	1.8634	$1.8634 \cdot 10^{15}$	−0.664
0.01	1.8640	$1.8640 \cdot 10^{10}$	−0.664
0.1	1.93	$1.93 \cdot 10^{5}$	−0.652
0.2	2.13	$6.66 \cdot 10^{3}$	−0.62
0.5	3.77	$1.21 \cdot 10^{2}$	−0.46
1	$1.22 \cdot 10$	$1.22 \cdot 10$	−0.256
5	$1.89 \cdot 10^{3}$	$6.05 \cdot 10^{-1}$	−0.0074
10	$5.84 \cdot 10^{4}$	$5.84 \cdot 10^{-1}$	−0.00092
20	$1.86 \cdot 10^{6}$	$5.81 \cdot 10^{-1}$	−0.00011

In the next section, an alternative form of the full nonlinear, though steady-state, film profile equation is examined.

Rising film flow

A liquid film is entrained by a solid substrate rising vertically from a pool of liquid, Figure 1b. The solid moves in the upward, negative x-direction at steady speed U, where U again is the unit of velocity measure. This situation was analyzed in the limit of high Reynolds number using film profile equations derived from integral balances by Cerro and Scriven (1979), and Kheshgi and Scriven (1979, see also Kheshgi, 1984). They report a match between their solution and experimental data. The alternative form of the film profile equation was used to predict a film thickness h_o which is similar, yet not identical, to that found by Cerro and Scriven (1979). Experimental data is not precise enough to discern whether or not the alternative form of the film profile equation is superior to that of Cerro and Scriven. In the next section, however, the exponential decay of film thickness h_o downstream is compared to exact solutions of the linearized Navier-Stokes system; the alternative form of film profile equation is found superior to that derived from integral balances.

In the applications of film profile equations which follow, the length scale ℓ and, therefore, the wavenumber α is not known *a priori*. The length ℓ is dependent on the parameters Re, St, Ca and g_i/g_j; therefore, the accuracy of the small wave-number expansion is dependent on these parameters. To allow application of film profile equations without appearance of the unknown α, film profile equation (Eq. 28) is recast with a single unit of length measure h_o.

A film profile equation for the steady profile of the film is given by viewing the film profile equation (Eq. 28) in a frame of reference stationary with respect to the liquid pool. Define coordinate $s \equiv x - t$. When recast in this coordinate and integrated once with respect to s, the film profile equation (Eq. 28) reduces to

$$q = h - \frac{h^3}{3}F + Re\left(-\frac{2}{15}h^5F_s - \frac{5}{24}h^4h_sF + \frac{37}{840}h^7FF_s + \frac{3}{40}h^6h_sF^2\right), \quad (41)$$

where

$$F = St + Ca^{-1}(2H)_s. \quad (42)$$

The flow rate of liquid carried upward by the liquid film measured in units of h_oU is:

$$q = 1 - St/3, \quad (43)$$

since the final downstream film thickness is the unit of length measure. The dimensional, final film thickness h_o, of course, is not known; finding the value of q is equivalent to finding h_o. Film profile equation (Eq. 41) can be recast by substituting F in the term multiplied by Reynolds number by the lowest order expression [the α order of terms in Eq. 41 is evident in the film profile equation (Eq. 28) before integration and before the choice of h_o as the single length scale]:

$$F = 3(h - q)/h^3, \quad (44)$$

to give

$$Ca^{-1}2H_s + St = \left(\frac{3}{h^2} - \frac{3q}{h^3}\right) + \frac{Re\,h_s}{5}\left(\frac{6}{7h} + \frac{6q}{7h^2} - \frac{54q^2}{7h^3}\right). \quad (45)$$

The lefthand side of Eq. 45 represents the driving forces of gravity and capillary pressure. The first term on the righthand side represents the effect of viscosity, the second the effect of inertia. This equation is of nearly identical form as the equation given by Kheshgi and Scriven (1979, see also Kheshgi, 1984) which was derived from a parabolic velocity profile and a momentum balance integrated over the film thickness:

$$Ca^{-1}2H_s + St = \left(\frac{3}{h^2} - \frac{3q}{h^3}\right) + \frac{Re\,h_s}{5}\left(\frac{1}{h} - \frac{6q^2}{h^3}\right). \quad (46)$$

For either Eq. 45 or 46, only one value of $q(Re, Ca)$ has been found (Kheshgi, 1984) to permit the equations to satisfy boundary conditions at the static meniscus in the liquid pool and the flat film downstream. Cerro and Scriven (1979) investigated the interesting limiting case of rapid rising film flows. They hypothesized (confirmed by solution of the film profile equation by the author 1984) that flux q and, therefore, the downstream film thickness h_o could be estimated, when Re is large, by requiring that inertia integrated over the film thickness be conserved and that viscous shear force balance the driving force of gravity—both at an internal layer where the film is of thickness δ. These two balances taken from the contents of Eq. 46 lead to

$$\delta^2 - 6q^2 = 0, \quad \delta^3 St - 3\delta + 3q = 0. \quad (47)$$

These equations yield Cerro and Scriven's fast coating limit

$$\delta = [3(1 - 6^{-1/2})]^{1/2}St^{-1/2} = 1.33238\ldots St^{1/2},$$
$$q = [(1 - 6^{-1/2})/2]^{1/2}St^{-1/2} = 0.54394\ldots St^{1/2}. \quad (48)$$

Comparisons to experimental data (Cerro and Scriven, 1979) proved this limit to be within the accuracy of the data. The film profile equation based on the long-wave expansion (Eq. 45) leads to a different conservation expression for inertia:

$$\delta^2 + \delta q - 9q^2 = 0, \quad (49)$$

and the same balance (Eq. 47) between gravity and viscous force. These equations yield a new fast coating limit

$$\delta = [3 - 6/(37^{1/2} - 1)]^{1/2} St^{-1/2}$$
$$= 1.34890 \ldots St^{1/2},$$
$$q = 2St^{-1/2}[3 - 6/(37^{1/2} - 1)]^{1/2}/(37^{1/2} - 1)$$
$$= 0.53078 \ldots St^{1/2}. \tag{50}$$

The result of these two different approaches are quite similar; data from rising film flow experiments do not show which is more accurate. In the next section the equations are again compared to exact results of linear analysis of the Navier-Stokes system to help determine the relative merits of the film profile equations.

Final acceleration of liquid films on moving substrates

When a liquid film is accelerated from, e.g., a coating device by a moving substrate, the film profile approaches exponentially a uniform film thickness, Figure 1c. Solutions of the linearized Navier-Stokes system in the absence of gravity ($St = 0$) calculated by Higgins (1980, 1982) become exact as the amplitude ϵ that the flow differs from a plug base flow becomes infinitesimal. Higgins (1980, 1982) found that far above the liquid bath the film profile is:

$$h = 1 + \epsilon e^{\lambda(Re,Ca)s}. \tag{51}$$

Selected values of growth rate λ found for vertical films are listed in Table 2. Film profile equations (Eqs. 41, 45 and 46) also predict an exponential growth of film thickness in the x direction far above the bath. Comparison of growth rates λ predicted by each film profile equation to Higgins' (1980, 1982) results, exact for infinitesimal disturbances, tests the accuracy of the three competing film profile equations.

As in the rising film flow case, there is no predetermined characteristic length ℓ of film development. In the small capillary number and small Reynolds number limit, however, the length of film development is known (see, e.g., Higgins 1982) to be asymptotically proportional to $Ca^{-1/3}$, and so the wave number of the flow in this limit is proportional to $Ca^{1/3}$. At higher Reynolds number, λ (a measure of the inverse of the characteristic length) is proportional to Re, Table 2. Hence, α is proportional to Re^{-1}, and so αRe is of $0(1)$ for large Re. It is expected that film profile equations based on a small wave-number expansion be asymptotically accurate as Ca decreases. It is seen below that the alternative form of the film profile equation is again accurate when inertia has a sizeable effect, i.e., when αRe is $0(1)$, as in the situation of disturbances to horizontal films.

The solution of each of the three profile equations when linearized to $h = 1$ is Eq. 51. The growth rate λ for Eqs. 41, 45 and 46 are, respectively, the roots of

$$Ca - \tfrac{2}{15} Re\lambda^4 - \tfrac{1}{3}\lambda^3 = 0, \tag{52}$$

$$Ca - \tfrac{2}{5} ReCa\lambda - \tfrac{1}{3}\lambda^3 = 0, \tag{53}$$

$$Ca - \tfrac{1}{3} ReCa\lambda - \tfrac{1}{3}\lambda^3 = 0. \tag{54}$$

Equations 53 and 54 each have three roots, and Eq. 52 has four. Of the roots, the smallest positive one is of the most interest and corresponds to the slowest growing disturbance in the s direction.

Reported in Table 2 are growth rates predicted by each of the three film profile equations: Eqs. 41, 45 and 46. When $Re = 0$, the three film profile equations are identical and growth rate $\lambda = (3Ca)^{1/3}$. The exact growth rate (Higgins, 1980, 1982) is only slightly less, when capillary number is 0.01 (the smallest capillary number Higgins listed), as can be seen in Table 2; the effect of streamwise viscous stresses that are neglected in film profile equations could account for the difference. Film profile equation (Eq. 45) parallels Higgins' results the closest, followed by Eq. 46 in which inertia does not affect growth rate as strongly as in Eq. 45. Comparison of Eq. 53 and 54 shows that film profile equation (Eq. 46) underestimates the effect of inertia by a factor of 5/6 compared to the alternative form (Eq. 45), which closely follows Higgins' exact results. Again, Eq. 42 compares poorly with Higgins' exact results, though it is asymptotically (as $\alpha \rightarrow 0$ or $Ca \rightarrow 0$, and $\alpha Re \rightarrow 0$)) identical to Eq. 45.

Table 2. Growth Rate for Final Acceleration to a Film on a Moving Substrate

Capillary No. Ca	Reynolds No. Re	Exact Solution	Growth Rate λ Approximate Profile Equations: 46	45	41
0.01	0	0.2936	0.310723	0.310723	0.310723
0.01	0.1	0.2925	0.309651	0.309436	0.309452
0.01	1	0.2817	0.3000	0.2978	0.2992
0.01	10	0.1829	0.2089	0.1915	0.2471
0.01	100	0.0246	0.0300	0.0250	0.1596
0.1	0	0.5287	0.66943	0.66943	0.66943
0.1	0.1	0.5241	0.6645	0.6635	0.6636
0.1	1	0.4860	0.6197	0.6099	0.6217
0.1	10	0.2185	0.2784	0.2387	0.4704
0.1	100	0.0246	0.0300	0.0250	0.2882
1	0	0.6969	1.44225	1.44225	1.44225
1	0.1	0.6884	1.4191	1.4145	1.4160
1	1	0.6143	1.2134	1.1689	1.2589
1	10	0.2249	0.2973	0.2487	0.8738
1	100	0.0246	0.0300	0.0250	0.5171

Film flow emerging from a slot coater

A liquid film is drawn by a moving substrate from the coating bead of a slot coater, as shown in Figure 1d. The finite amplitude decay of film thickness has been studied by Silliman (1979), and Saito and Scriven (1981) by direct solution of the Navier-Stokes system by the finite element method. Their solutions, however, do not cover the regime over which the alternative form of the film profile equation is expected to be accurate and where its accuracy is to be tested, i.e., small Ca over a range of Re. [The smallest capillary number Saito and Scriven (1981) report, when Re is nonzero, is $Ca = 0.125$.] Film profile equations have previously not been used to approximate film profiles for this flow when Re is nonzero.

Film profile equation (Eq. 45), in the absence of gravity ($St = 0$), describes the finite amplitude development of the emerging film. This equation is solved by shooting (numerical integration) from its asymptotic solution far downstream, described by Eq. 51, to the mouth of the slot at $s = 0$. The unit of length measure h_o is taken to be the final film thickness. Slot width $d = 1/0.07 = 14.29$ times the final film thickness h_o, $Ca =$

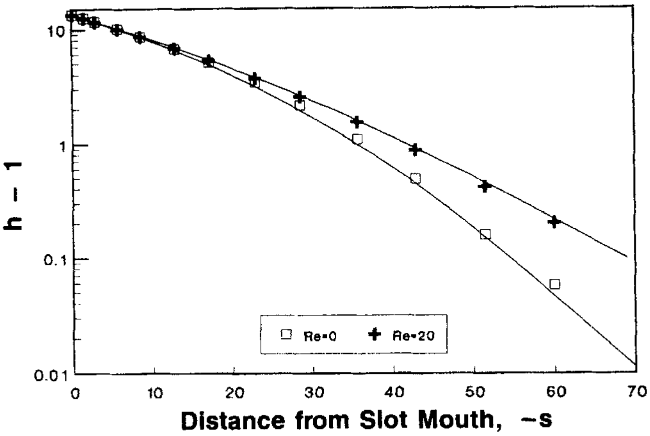

Figure 3. Finite-amplitude decay of film thickness of a film emerging from a slot coater.

0.001 and $Re = 0$ or 20. These parameters are chosen to be a test of the finite-amplitude film development in the regime of small wave number and moderate Reynolds number. Calculated profiles for these two cases are shown by the solid curves in Figure 3.

Solutions calculated by means of the penalty/Galerkin finite element method (Kheshgi and Scriven, 1984) are used to stand in the place of exact solutions for the two choices of parameters. A mesh of 3 by 21 biquadratic-velocity, linear-pressure elements provide sufficient accuracy. The algorithm was successfully tested by reproducing Saito and Scriven's (1981) results. Solution at $Re = 20$ (which is equivalent to a Reynolds number defined by Saito and Scriven of $20/0.07 = 285.7$) required continuation from solutions at lower Reynolds numbers. Calculated film thickness values at element nodes are shown by the symbols in Figure 3.

Figure 3 shows the finite amplitude decay of film thickness from the slot mouth ($s = 0$), through a region of finite-amplitude decay, to an exponential decay to the final (unit) film thickness. The nonexponential decay of film thickness evident by the bend in the curves on the semilog plot is due to finite amplitude effects. In the $Re = 20$ case, solution of the film profile equation (Eq. 45) differs from the finite element solution by less than 1% over the region of film greater than one slot width d downstream ($s < -d$) from the slot mouth ($s = 0$). At $s = -d$, the film thickness $h = 7.8$ times the final film thickness, definitely in the finite-amplitude regime. Within one slot width of the slot mouth ($-d < s < 0$), the two solutions disagree by less than 4% due to the rearrangement of the velocity field from that within the slot coater ($s > 0$) to that in the film ($s < 0$), a rearrangement which film profile equations are not expected to reproduce. At this capillary number, solutions of the alternative form of the film profile equation have sufficient accuracy for engineering applications.

Discussion and Generalization

An alternative form of film profile equation (Eq. 28) is found in each of the four cases in the preceding section to lead to solutions of high accuracy over a wide range of Reynolds numbers. To arrive at the alternative form, the film profile equation of lowest-order accuracy (Eq. 17) is used to substitute terms in the next order expression, keeping the same asymptotic order of accuracy, yet improving the accuracy of the result when the effect of inertia is sizable. This phenomenon in asymptotic analyses appears over and over again in different applications, but not always for obvious reasons. The opportunity to exchange time and space derivatives in film profile equations used to study disturbances to flow down inclined films was noted by Atherton and Homsy (1976), but without any explanation of the reason for doing so. This approach was found useful by Benjamin et al. (1972) in extending the KdV equation to include finite wavenumber effects. Unusual in the derivation of the *alternative* form (Eq. 45) of the film profile equation is that no small-amplitude approximation is made, unlike that made in the derivation of the KdV equation. An explanation of the improved accuracy of the alternative forms found in the comparisons is now attempted.

The correction to film profile equation (Eq. 17) that accounts for the effect of inertia Eqs. 23 and 27 is given by

$$-\left(\int_0^h \alpha u^{(1)}\,dy\right)_x = -\alpha Re \cdot \left\{\int_0^h \int_0^y \int_h^y [u_t^{(0)} + u^{(0)}u_x^{(0)} + v^{(0)}u_y^{(0)}]\,dy^3\right\}_x . \quad (55)$$

The approximate profile $u^{(0)}$ contains an error of $0(\alpha^2 + \alpha Re)$. Using it in Eq. 55 results in an error in that expression of $0(\alpha^2 Re^2 + \alpha^3 Re)$. When αRe becomes large, so does the error causing grossly inaccurate solutions such as those given in Tables 1 and 2. An interpretation of the substitution used to arrive at the alternative form is that the exact expression of the x gradient of volumetric flux given by the integral form of the kinematic condition (Eq. 4) is used to approximate the triple integral of the velocity expression Eq. 55. For small-amplitude, long disturbances the difference between the single integral of the time derivative of Eq. 4 and the triple integral is a constant of proportionality K related to the y profile of velocity u, not its magnitude, i.e.

$$h_{tt} = -\left(\int_0^h u\,dy\right)_{tx} = -K\left(\int_0^h \int_0^y \int_h^y u_t\,dy^3\right)_x . \quad (56)$$

The value of K, seen in Eq. 37, is $-5/2h^2$, based on parabolic velocity profile (Eq. 17). The exact velocity profile is, of course, a function of Reynolds number; e.g., at high Reynolds number the appropriate velocity profile is plug flow (cf. Whitham, 1974) and results in $K = -3/h^2$. As αRe becomes large, however, the error in the estimate in K does not grow like αRe, as it does at small Reynolds number, but rather is bound to be no larger than $0(1)$. The implication is, that if Eq. 56 is used to substitute terms in Eq. 55, at least for small amplitude, the error in term (Eq. 55) does not grow unbounded as αRe becomes large, but rather becomes $0(\alpha Re)$, the same order as the lefthand side of Eq. 55. This leads to the accurate, yet not asymptotic, solutions seen in the preceding section.

In general, the alternative form of film profile equation (Eq. 28) can be derived by replacing x derivatives of F using Eq. 19. For steady film flows or the evolution of small-amplitude disturbances, as demonstrated in the applications above, this results in no appearance of driving force F in inertia term (Eq. 55) in the alternative form of the film profile equation. For transient film profile equations, however, after the replacement terms containing F and F_t remain in nonlinear elements of the inertia term; what this implies concerning the accuracy of finite-amplitude, moderate-Reynolds-number, unsteady, film-profile solutions is unresolved. The appearance of F and F_t could also be removed by first approximating the inertia term by a small-amplitude expansion—keeping only dominant nonlinear terms—as Whitham (1974) shows is done in the derivation of the KdV equation. The expectation, of course, is that these terms will not affect the accuracy of solutions since accuracy has been demonstrated for infinitesimal-amplitude, moderate-Reynolds-number, unsteady film flows and for finite-amplitude, moderate-Reynolds-number, steady, film flows.

Conclusions

A film profile equation is derived which is asymptotically accurate at small wave number and Reynolds number, and is found to be accurate—although not asymptotically so—for small wave number and arbitrary Reynolds number. Accuracy is demonstrated in comparison with exact solutions of the Navier-Stokes equations for infinitesimal disturbances to horizontal films, final acceleration of moving films, emerging flow out of a slot coater, and with approximate solutions for steady flow of entrained films rising from a liquid bath. This equation is useful in analysis of film flow situations where disturbances are of greath length and finite amplitude, and where the effect of inertia can be sizable.

Notation

$Ca = \mu U/\sigma$, capillary number
d = slot width measure in units of final film thickness
F = driving force defined by Eq. 18
g = acceleration of gravity
g_i = x component of the unit gravity vector
g_j = y component of the unit gravity vector
h = film thickness
h_o = characteristic film thickness
H = mean curvature of free surface
K = velocity-profile-dependent constant
ℓ = characteristic length in x direction
p = pressure
q = flow rate
$Re = \rho U h_o/\mu$, Reynolds number
$s = x - t$, coordinate in a frame stationary with liquid pool
$St = h_o^2 \rho g/\mu U$, inverse Stokes number
t = time
U = characteristic velocity
u,v = Cartesian components of velocity
x,y = Cartesian coordinates tangent and normal to film substrate

Greek letters

$\alpha = h_o/\ell$, dimensionless wavenumber
δ = film thickness at internal layer for rapid rising film flow
ϵ = amplitude
γ = defined by Eq. 30
λ = growth rate
μ = viscosity
ρ = density
σ = surface tension

Superscripts

( ) = order of wavenumber expansion
$'$ = dimensional variable

Literature Cited

Airy, S. G. B., "Tides and Waves," *Encyc. Metrop. Art.*, **192** (1845).
Atherton, R. W., and G. M. Homsy, "On the Derivation of Evolution Equations for Interfacial Waves," *Chem. Eng. Commun.*, **2**, 57 (1976).
Benjamin, T. B., J. L. Bona, and J. J. Mahony, "Model Equations for Long Waves in Nonlinear Dispersive Systems," *Phil. Trans. R. Soc. Lond.*, **A278**, 555 (1972).
Benney, D. J., "Long Waves on Liquid Films," *J. Math. Phys.*, **45**, 150 (1966).
Boussinesq, J., "Theorie de L'intumescence Liguide Appelee onde Solitaire ou de Translation se Propageant dans un Canal Rectangulaire," *Comptes Rendus*, **72**, 755 (1871).
Cerro, R. L., and L. E. Scriven, "Rapid Free Surface Film Flows: an Integral Approach," *I&EC Fund.*, **19**, 40 (1979).
Esmail, M. N., and R. L. Hummel, "Nonlinear Theory of Free Coating onto a Vertical Surface," *AIChE J.*, **21**, 958 (1975).
Gauglitz, P. A., and C. J. Radke, "An Extended Evolution Equation for Liquid Film Breakup in Cylindrical Capillaries," *Chem. Eng. Sci.*, **43**, 1457 (1988).
Gjevik, B., "Occurrence of Finite-amplitude Surface Waves on Falling Liquid Films," *Phys. Fluids*, **13**, 1918 (1970).
Higgins, B. G., "Capillary Hydrodynamics and Coating Beads," PhD Thesis, Univ. of Minnesota, Minneapolis (1980).
———, "Downstream Development of Two-dimensional Visco-capillary Film Flow," *I&EC Fund.*, **21**, 168 (1982).
Higgins, B. G., and L. E. Scriven, "Interfacial Shape and Evolution Equations for Liquid Films and other Viscocapillary Flows," *I&EC Fund.*, **18**, 208 (1979).
Kheshgi, H. S., "The Motion of Viscous Liquid Films," PhD Thesis, Univ. of Minnesota, Minneapolis (1984).
Kheshgi, H. S. and L. E. Scriven, "Rising Film Flow: First-order Approximation Solved," *Bull. of the Amer. Phys. Soc.*, **24**, 1131 (1979).
Kheshgi, H. S. and L. E. Scriven, "Penalty Finite Element Analysis of Unsteady Free Surface Flows," *Finite Elements in Fluids*, **5**, 393, ed., R. H. Gallagher et al., Wiley, New York (1984).
Kheshgi, H. S., and L. E. Scriven, "The Evolution of Disturbances in Horizontal Films," *Chem. Eng. Sci.*, **43**, 793 (1988).
Korteweg, D. J., and G. deVries, "On the Change of Form of Long Waves Advancing in a Rectangular Channel, and on a New Type of Long Stationary Wave," *Phil. Mag.*, **39**(5), 422 (1895).
Krantz, W. B., and S. L. Goren, "Finite-amplitude, Long Waves on Liquid Films Flowing Down a Plane," *I&EC Fund.*, **9**, 107 (1970).
Lamb, H., Hydrodynamics, Dover Publications, New York (1945).
Landau, L., and B. Levich, "Dragging of a Liquid by a Moving Plate," *Acta Physicochim U.R.S.S.*, **17**, 42 (1942).
Nakaya, C., "Long Waves on a Thin Fluid Layer Flowing Down an Inclined Plane," *Phys. Fluids*, **18**, 1407 (1975).
Orchard, S. E., "On Surface Levelling on Viscous Liquids and Gels," *Appl. Sci. Res.*, **11**, 451 (1962).
Petviashvili, W. I., and O. Yu. Tsvelodub, "Horseshoe-shaped Solutions on a Flowing Viscous Film of Fluid,"*Sov. Phys. Dokl.* English translation, **23**, 117 (1978).
Roskes, G. J., "Three-dimensional Long Waves on a Liquid Film," *Phys. Fluids*, **13**, 1440 (1970).
Ruschak, K. J., "Flow of a Falling Film into a Pool," *AIChE J.*, **24**, 705 (1978).
Saito, H., and L. E. Scriven, "Study of Coating Flow by the Finite Element Method," *J. Comp. Phys.*, **42**, 53 (1981)
Silliman, W. J., "Viscous Film Flows with Contact Lines: Finite Element Simulation, a Basis for Stability Assessment and Design Optimization," PhD Thesis, Univ. of Minnesota, Minneapolis (1979).
Spiers, R. P., C. V. Subbaraman, and W. L. Wilkinson, "Free Coating of a Newtonian Liquid onto a Vertical Plate," *Chem Eng. Sci.*, **29**, 389 (1974).
Tallmadge, J. A., and A. J. Sorka, "The Additional Parameter in Withdrawal," *Chem. Eng. Sci.*, **24**, 377 (1969).
Teletzke, G. F., "Thin Liquid Films: Molecular Theory and Hydrodynamic Implications," PhD Thesis, Univ. of Minnesota, Minneapolis (1983).
Whitham, G. B., "Linear and Nonlinear Waves," New York (1974).
Wehausen, J. V., and E. V. Laitone, "Surface Waves," *Handbuch der Physik*, ed., S. Flugge, **9**, 446 (1960).

Manuscript received Jan. 26, 1989, and revision received July 21, 1989.